Original scientific paper

https://doi.org/10.33180/InfMIDEM2019.106

Informacije MIDEM
Journal of Microelectronics,
Electronic Components and Materials
Vol. 49, No. 1(2019), 43 – 50

Optimization of shunt capacitive RF MEMS switch by using NSGA-II algorithm and uti-liti algorithm

Alireza.Ardehshiri[1], Gholamreza Karimi[2], Ramin Dehdasht-Heydari[1]

[1]Islamic Azad University, Department of Electrical Engineering, Kermanshah Branch, Kermanshah, Iran
[2]Razi University, Faculty of Engineering, Department of Electrical Engineering, Kermanshah, Iran

Abstract: The present paper aimed at designing, optimizing, and simulating the RF MEMS Switch which is stimulated electrostatically. The design of the switch is located on the CoplanarWaveguide (CPW) transmission line. The pull-in voltage of the switch was 2V and the axial residual stress of the proposed design was obtained at 23MPa. In order to design and optimize the geometric structure of the switch, the desired model was extracted based on the objective functions of the actuation voltage and the return loss up-state and also the isolation down-state using the mathematical programming. Moreover, the model was solved by the NSGA-II meta-heuristic algorithm in MATLAB software. In addition, the design requirements and the appropriate levels for designing the switch were obtained by presenting the Pareto front from the beam actuation voltage and also the return loss up-state and isolation down-state. Finally, the RF parameters of the switch were calculated as S11=-2.54dB and S21=-33.18dB at the working frequency of 40GHz by extracting the appropriate parameters of the switch design through simulating a switch designed by the COMSOL Multiphysics software 4.4a and the advanced design system (ADS).

Keywords: RF switch MEMS; Genetic algorithm; uti-liti algorithm; Actuation voltage

Optimizacija šarazitne kapacitivnosti RF MEMS stikala z uporabo algoritmov NSGA-II in uti-liti

Izvleček: Članek predstavlja načrtovanje, optimizacijo in elektrostatično simulacijo RF MEMS stikala. Dizajn stikala je osnovan na CPW prenosni liniji. Za optimizacijo structure stikala so bile uporabljene objektivne funkcije aktuacije napetosti, povratnih izkub v vzbijenem stanju in izolativnosti v izklopljenem stanju. Model je bil rešen z NSGA-II metahevrističnem modelu v MATLABu. Izračunani RF parametri stikala pri delovni frekvenci 40 MHz znašajo S11=-2.54dB in S21=-33.18dB. Parametri so bili določeni s pomočjo COMSOL Mutiphysics programske opreme.

Ključne besede: RF MEMS stikala; generični algoritem; uti-liti algoritem; aktuacijska napetost

** Corresponding Author's e-mail: ghrkarimi@yahoo.com*

1 Introduction

The Micro-Electromechanical System (MEMS) refers to a technological process used to create integrated systems and components of the complex (or the combination of the electrical and mechanical elements) [1]. In this regard, the MEMS switches are significantly considered due to their efficiency in areas such as fuzzy array systems and switching filters for wireless communication.[2] MEMS switches have low power consumption, very high isolation, very low insertion loss (the RF MEMS switches have the insertion loss of about 0.1 to 100 GHz) and high linear performance as compared to the diodes or FET switches[3]. However, the high actuation voltage and the high switching time are among the weaknesses of the MEMS switches. MEMS switches are of different types, in which series of switches (ohm connection) and parallel switches (capacitance) have various applications. In this sense, they can be used as an ohm (serial switches) and also the capacitive switch (shunt switches) using electrostatic, electromagnetic ,piezoelectric or thermal designs[3]. The electrostatic setup is usually used due to its power consumption closed to zero, lower performance time, and smaller size [2]. MEMS switches can be used both on micro strip lines and CPW lines of the glass, silicon and GaAs substrates, which are capable of being operated in these configurations up to the frequency of 100 GHz. A dielectric layer has been used in contacting the switch with the transmission line to prevent corrosion and fatigue in metal-to-metal connection [2]. It is worth mentioning that important parameters should be considered in designing MEMS switches. These parameters include the electrostatic actuation voltage, isolation, transmission losses, and operating time[2]. Numerous studies have been conducted on the evaluation of the performance of MEMS switch and its important parameters. As a switch is presented in [4], the return loss of -5.6 dB and an isolation of -24.38dB are obtained from an output voltage of 3.04 V and at a frequency of 40 GHz, using the design of the experiment of. When a switch is presented in[5], the return loss of -3.1dB and an isolation of -15dB are obtained from an output voltage of 7V and at a frequency of 40GHz. When a switch is presented in[6], the return loss of -0.98 dB and an isolation of -17.9dB are obtained from an output voltage of 82V and at a frequency of 20 GHz. Besides, when a switch is presented in[7], the return loss of -0.68 dB and an isolation of -35.78dB are obtained from an output voltage of 23.6V and at a frequency of 40 GHz. Moreover, when a switch is presented in[8], the return loss of -0.8 dB and an isolation of -30dB are obtained from an output voltage of 25V and at a frequency of 40 GHz. Finally, when a switch is presented in [9], from an output voltage of 3V and at a frequency of 40 GHz, using the design of the experiment of. In the present paper, a suitable model was extracted for optimizing the multi-object in the target functions (voltage actuation and RF parameter) of the switch using the mathematical programming method. Then, the proposed model was solved using the NSGA-II[1] meta-heuristic algorithm. In addition, the proposed model was used to achieve a MEMS switch with low electrostatic actuation voltage and improved insertion loss and isolation by choosing the proper structures of width, length, and thickness and, also, using the Pareto front presented for the designed beam spring constant.

The present paper is organized as follows: Section 2 evaluates the switch performance. Section 3 examines the details of the model and presents the Pareto front solution set for the actuation voltage and return loss up-state and isolation down-state by solving the proposed model using the NSGA-II in MATLAB software and the uti-liti algorithm. Finally, section 4 simulates the desired switch using the COMSOL and ADS software and evaluates the necessary parameters such as actuation voltage, operating time, insertion loss and the isolation.

[1] *Non-dominated Sorting Genetic Algorithm-II*

2 MEMS switches performance

2.1 Initial performance

Fig.1 illustrates a parallel MEMS switch. Which is located on the coplanar waveguide and includes two electrodes. The lower electrode is the central transmission line of the waveguide, while the upper electrode is a thin metal sheet, which is suspended on the lower electrode and connected to the lateral conductors of the coplanar waveguide. Further, the thin dielectric layer is covered on the lower electrode to prevent the metal-to-metal connection [10]. In the state up with the bridge in up position, the switch is OFF and shows insertion loss. ON state can be achieved by pulling down the beam in the down position through electro-static actuation. The isolation state is occurred especially when the bridge provides the ground for the float central capacitive area. The electrostatic actuation voltage of the capacitance switches is calculated according to the equation 1:[2]

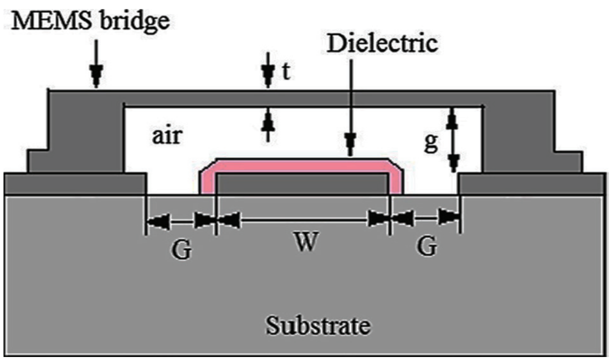

Figure 1: The schematic of the switch

$$V = V\left(\frac{2}{3}g_0\right) = \sqrt{\frac{8k}{27\varepsilon_0 A}g_0{}^3} \quad (1)$$

Where ε_0 represents the vacuum permittivity coefficient and indicates the air gap between the suspended bridge and the transmission line, the electrostatic actuation voltage is zero, and shows the beam spring constant. As shown in the equation, the distance ($g_0 = g_{gap} + thd$) and the area of the switch (A) can be reduced in order to achieve a low spring constant. The S-parameters are first measured in the up-state position data (S_{11}) which is fitted to get the up-state capacitance of the switch. S_{11} is achieved using the equation 2. The S-parameters are first measured in the down-state position data (S_{21}) which is fitted to get the up-state capacitance of the switch. $S_{21}$is achieved using the equations 3 .[11]magnetostatic, piezoelectric, or thermal designs. To\\ndate, only electrostatic-type switches have been demonstrated at 0.1-100\\nGHz with high reliability (100 million to 10 billion cycles

$$S_{11}\left(\text{up state}\right)\simeq\frac{-j\omega c_u z_0}{2+j\omega c_u z_0}\Rrightarrow$$
$$\Rrightarrow\left|S_{11}{}^2\right|\simeq\frac{\omega^2 Z_0{}^2\left(\varepsilon_0 Ww\right)^2}{4\left(g_{gap}+\left(\frac{t_d}{\varepsilon_r}\right)\right)^2} \tag{2}$$

$$S_{21}\left(\text{down state}\right)\simeq\frac{2}{2+j\omega c_d z_0}\Rrightarrow$$
$$\Rrightarrow\left|S_{21}{}^2\right|\simeq\frac{4t_d{}^2}{\omega^2 Z_0{}^2\left(\varepsilon_0\,\varepsilon_r\,Ww\right)^2} \tag{3}$$

Where Z_0 implies the impedance of the transmission line which is equal to 50 Ohms, ω is the angular frequency and the C_u and C_d of the capacitor are in up-state and down-state and the C_u and $C_d$are achieved using the equations 4.1 and 4.2:

$$C_d=\frac{\varepsilon_0\varepsilon r Ww}{t_d} \tag{4.1}$$

$$C_u=\frac{\varepsilon_0 Ww}{g_{gap}+\left(\frac{t_d}{\varepsilon_r}\right)} \tag{4.2}$$

3 RF MEMS switch design

3.1 Principles for mathematical programming

Mathematical programming is based on the problem modelling. In other words, the programming techniques are used to achieve the maximum efficiency and the right decision-making process in terms of optimization and efficiency. Generally, the research techniques in operation are categorized in accordance to observation, definition, modelling, model solving, and model implementing, which should be considered in order to obtain the results of the research. [12] in a mathematical programming technique, four main and important parts should be followed in order to create a proper model of the problem. The objective function, constraints, decision variables, and parameters are the principles for designing a model using the mathematical programming. The solution set of the objective function is called the Pareto front, which is an optimal vector dominating other vectors especially when no similar vectors can be found in the entire solution space.[12] In this sense, the vector is generally called the non-dominated answer, and the set of these points is called the Pareto Front[13]. In order to optimize RF switch MEMS, A multi-objective integer programming model is proposed. The proposed model includes three objective functions: minimizing the actuation voltage and minimizing the return loss up-state and maximizing isolation down-state. Descriptions of objective function, constraints, decision variables, and parameters of the mathematical model are presented in Table 1.

3.2 Objective functions

The objective functions are to minimize the actuation voltage, maximize the isolation and minimize the return loss as defined below:

- Minimizing the actuation voltage. The objective function for actuation voltage is based on the equation (1).
- Minimizing the return loss up-state for the best isolation. The objective function for return loss is based on the equation. (2).
- Maximizing the isolation down-state. The objective function for isolation is based on the equation (3).

The model presented in this paper is shown in equation 5.

Table 1: List of parameters , and decision variables

Parameters				
AL Young's modulus (E)	AL Poisson's ratio (ν)	Switch thickness (t)	Frequency of operation (f)	Switch Width(w)
70GPa	0.32	0.877µm	40GHz	80µm
Decision variables				
Spring constant (k)	Switch Length (W)	Dielectric layer thickness (t_d)	Air gap (g_{gap})	

$$Actuation\,voltage:\ \min: Z1 = \ V = \sqrt{\frac{8k}{27\varepsilon_0 Ww} g_0^{\ 3}}$$

$$Return\,loss\,up-state: Min: \ \ Z2 = \left|S_{11}\right|^2 \simeq \frac{\omega^2 Z_0^{\ 2}\left(\varepsilon_0 Wv\right.}{4\left(g_{gap} + (\frac{t_d}{\varepsilon_r}\right.} \quad (5)$$

$$Isolation\,down-state: Max: Z3 = \left|S_{21}\right|^2 \simeq \frac{4t_d^{\ 2}}{\omega^2 Z_0^{\ 2}\left(\varepsilon_0 \varepsilon_r W\right.}$$

subject.to:

$$\begin{cases} 1N/m \le k \le 1.4N/m \\ 150\mu m \le W \le 200\mu m \\ 1.1\mu m \le g_{gap} \le 1.4\mu m \\ 0.085\mu m \le t_d \le 0.11\mu m \end{cases}$$

3.3 Genetic algorithm

In order to solve the proposed multi-objective model and determine the decision variables, we used the NSGA-II algorithm. It is an evolutionary algorithm by which one is able to find sets of optimal solutions on Pareto-optimal fronts. It has been developed as an efficient algorithm to solve multi-objective optimization problems [14]. The best values for the algorithm's parameters are defined in Table 2.

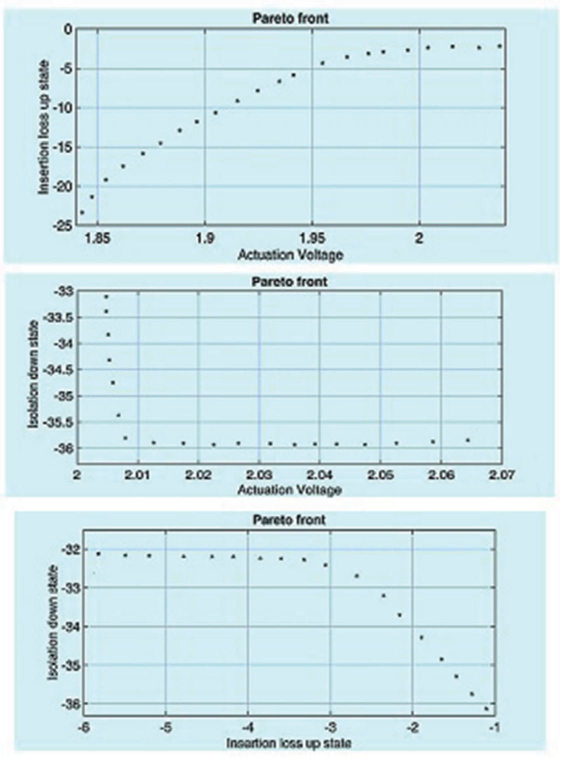

Figure 2: The visualization of the estimates of the Pareto front for the case study problem.

Table 2: Best parameters for NSGA-II algorithm

Population size	Number of iteration	Crossover probability (Pc)	Mutation (Pm)
250	500	0.8	0.25

After tuning the NSGA-II parameters, the model RF switch MEMS problem is solved in MATLAB software. The visualization of the estimates of the Pareto front for the case study problem is depicted in Fig. 2.

The values of target functions and variables are shown using the algorithm NSGA-II in Table 3.

Table 3: The values of target functions and variables

n	V	S_{11}	S_{21}	k	W	g_{gap}	t_d
1	1.981	-2.985	-32.417	1.333	199.841	1.115	0.094
2	2.03	-2.856	-33.209	1.442	199.956	1.109	0.087
3	1.421	-2.756	-34.110	1.214	199.969	1.118	0.085
4	2.032	-2.569	-33.593	1.389	199.946	1.121	0.084
5	2.051	-2.498	-33.124	1.398	199.898	1.131	0.091
6	2.026	-2.897	-34.459	1.445	199.995	1.141	0.93
7	1.996	-2.654	-34.158	1.498	199.972	1.131	0.087
8	2.019	-2.756	-33.275	1.245	199.964	1.115	0.088
9	2.015	-2.236	-34.163	1.469	199.997	1.154	0.091
10	2.062	-2.479	-33.231	1.326	199.963	1.112	0.087
11	1.992	-2.569	-33.195	1.213	199.979	1.104	0.084
12	2.113	-2.897	-34.189	1.335	199.854	1.106	0.088
13	2.057	-2.746	-34.356	1.456	199.897	1.109	0.087
14	2.067	-2.663	-34.237	1.364	199.964	1.103	0.086
15	2.042	-2.789	-34.187	1.287	199.985	1.110	0.088
16	2.034	-2.567	-33.598	1.251	199.932	1.113	0.089
17	2.031	-2.859	-34.320	1.199	199.987	1.112	0.087
18	2.019	-2.669	-33.365	1.203	199.935	1.155	0.092

3.4 Utiliti algorithm

It is clear that each set of the solutions represents a scenario for the development of a capacitance switch. Considering the same preference for the solutions obtained in the answer set, the approach based on the uti-liti of the target functions was used to find the optimal answer in such a way that each of the target functions has the least distance from the best value in the answer reported as the optimal one. In the approach used to select the answer from the set of solutions, the Equation 6.1 should be optimized in such a way that the Ui related to the uti-liti of the target function can be equal to Zi. Given the equations 6.2-6.5.[15], the uti-liti value is equal to the one for conditions in which each target function has its best value, while the uti-liti value is zero for conditions in which the target function has its worst possible value. [16]

$$\max \gamma \tag{6.1}$$

$$\gamma = \min\left(U_1, U_2, U_3\right) \tag{6.2}$$

$$U_1 = \left(\frac{Z_1^{max} - Z_1}{Z_1^{max} - Z_1^{min}}\right) \tag{6.3}$$

$$U_2 = \left(\frac{Z_2^{max} - Z_2}{Z_2^{max} - Z_2^{min}}\right) \tag{6.4}$$

$$U_3 = 1 - \left(\frac{Z_3^{max} - Z_3}{Z_3^{max} - Z_3^{min}}\right) \tag{6.5}$$

Table 4 presents the values related to the best, worst, and final values of the target function in the selected answer. According to the proposed uti-liti algorithm, the appropriate values for the actuation voltage and the return loss up-state and the isolation down-state values are equal to V=1.992V, S_{11}=-2.569dB, S_{21}=-33.195dB.

The optimal answer for the switch is obtained in row 11. According to the proposed algorithm, the optimal switch design is presented in the Table 5.

3.5 Switch spring constant

The spring constant presented in equation 7 is obtained with the design of spiral beams as shown in Fig.3[17]

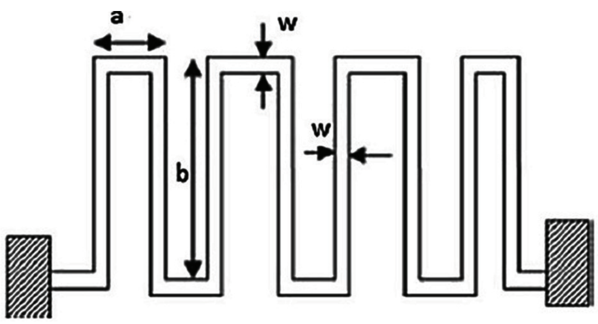

Figure 3: Spiral Beams Design

Table 4: Final value of the target function

n	V	S11	S21	U1	U2	U3	γ
1	1.981	-2.985	-32.417	0.1907514	0	1	0
2	2.03	-2.856	-33.209	0.1199422	0.17223	0.612145	0.119942
3	1.421	-2.756	-34.110	1	0.305741	0.170911	0.170911
4	2.032	-2.569	-33.593	0.117052	0.555407	0.424094	0.117052
5	2.051	-2.498	-33.124	0.0895954	0.6502	0.653771	0.089595
6	2.026	-2.897	-34.459	0.1257225	0.11749	0	0
7	1.996	-2.654	-34.158	0.1690751	0.441923	0.147405	0.147405
8	2.019	-2.756	-33.275	0.1358382	0.305741	0.579824	0.135838
9	2.015	-2.236	-34.163	0.1416185	1	0.144956	0.141618
10	2.062	-2.479	-33.231	0.0736994	0.675567	0.601371	0.073699
11	1.992	-2.569	-33.195	0.1748555	0.555407	0.619001	0.174855
12	2.113	-2.897	-34.189	0	0.11749	0.132223	0
13	2.057	-2.746	-34.356	0.0809249	0.319092	0.050441	0.050441
14	2.067	-2.663	-34.237	0.066474	0.429907	0.108717	0.066474
15	2.042	-2.789	-34.187	0.1026012	0.261682	0.133203	0.102601
16	2.034	-2.567	-33.598	0.1141618	0.558077	0.421645	0.114162
17	2.031	-2.859	-34.320	0.1184971	0.168224	0.068071	0.068071
18	2.019	-2.669	-33.365	0.1358382	0.421896	0.535749	0.135838

Table 5: Optimal switch design

n	V	S11	S21	U1	U2	U3	γ
11	1.992	-2.569	-33.195	0.174855	0.555407	0.619001	0.174855
Variables							
k		W		ggap		td	
1.213		199.979		1.104		0.084	

$$k_z = \left[\left[\frac{\left(8N^3a^3\right)+\left(2Nb^3\right)}{3EI_x} + \frac{abN\left[3b+(2N+1)(4N+1)a\right]}{3G_j} \right] - \left[\frac{Na^2\left[\left(\frac{2Na}{EI_x}\right)+\frac{(2N+1)b}{G_j}\right]^2}{2\left(\frac{a}{EI_x}+\frac{b}{G_j}\right)} - \frac{Nb^2}{2}\left(\frac{a}{G_j}+\frac{b}{EI_x}\right) \right] \right]^{-1} \quad (7)$$

Table 6 presents the parameters of equation (7).

Table 6: The parameters of the equation (7)

Primary meander length (a)	Secondary meander length (b)	Beam with	Shear module (G_j)
4.5µm	45µm	1.7µm	E/(2(1+ν))
x-axis moment of inertia (Ix)	z-axis moment of inertia (Iz)	Polar moment of inertia (Ip)	Torsion constant (J)
$wt^3/12$	$wt^3/12$	Ix+Iz	$0.413I_P$

4 Designed switch analysis

After optimizing the suggested switch using the genetic algorithm and uti-liti algorithm presented in the previous sections, the electrical and mechanical properties and the efficiency of the RF MEMS parallel switch are optimized and simulated using COMSOL Multiphysics 4.4a and Advance Design System (ADS). Finally, the response provided by the parallel switch is reviewed.

4.1 Electro-Mechanic Analysis

The design and the optimization of the switch were investigated. The proposed design was simulated in the COMSOL software. The boundary conditions used in this design include fixing the end of the beam, applying zero voltage to the dielectric subsurface, applying the bias voltage to the membrane surface, applying symmetry conditions, using boundary load conditions to the beam subsurface to prevent infinite displacement error, and applying the boundary conditions of the electrical DC voltage on the switch level. Fig.4 illustrates the simulation results of the designed optimal switch. It is observed that applying the actuation voltage of 2V to the surface of the membrane causes a displacement of 1.1 µm and reaches the transmission line voltage to zero. Figs.4.a and 4.b illustrate the results obtained from the displacement and the axial residual stress. The axial residual stress resulting from applying the voltage to the switch surface is equal to σ=23MPa.

(a)

(b)

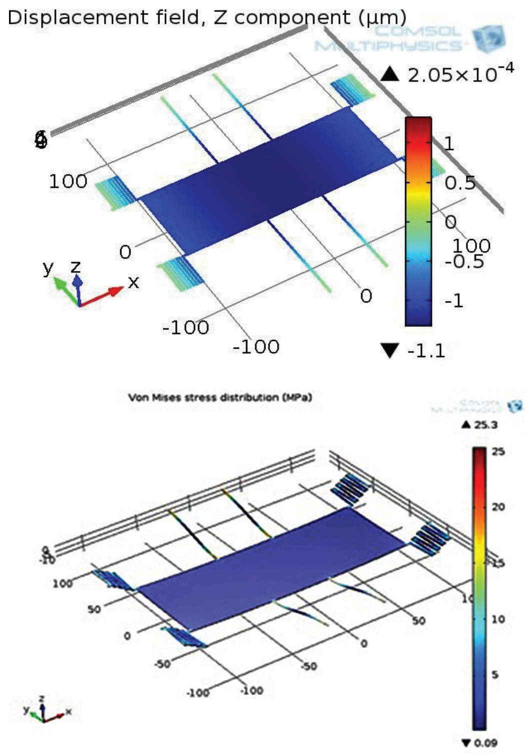

Figure 4: (a) Z-displacement distribution and (b) Von Misses stress distribution

4.2 Switch operation time and capacitor variations

The switch operation time which is highly dependent on the voltage is applied to the beam membrane. The response time is about 29.6µs by designing an optimal

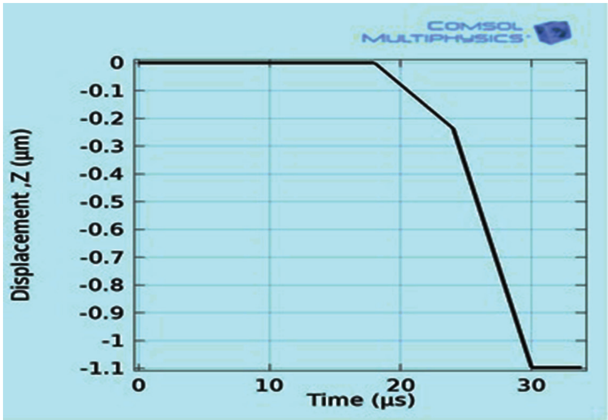

Figure 5: Simulation of the optimized RF-MEMS switch in time domain. Membrane's movement

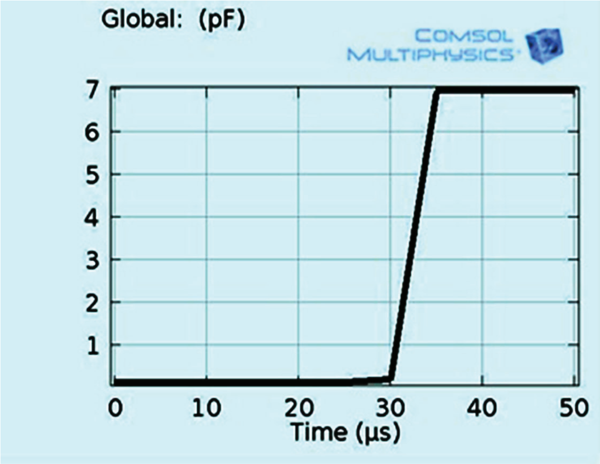

Figure 6: Capacitances of switch-on and switch-off

switch and applying the electrostatic actuation voltage as illustrated in Fig.5. Besides, it is possible to obtain the quickest answers by increasing the actuation voltage. As a result, the amount of capacitor is obtained at about 7pF after applying the electrostatic actuation voltage to the switch. When the electrostatic actuation voltage is cut off, the value of the capacitor is equal to 0.1 pF as shown in Fig.6.

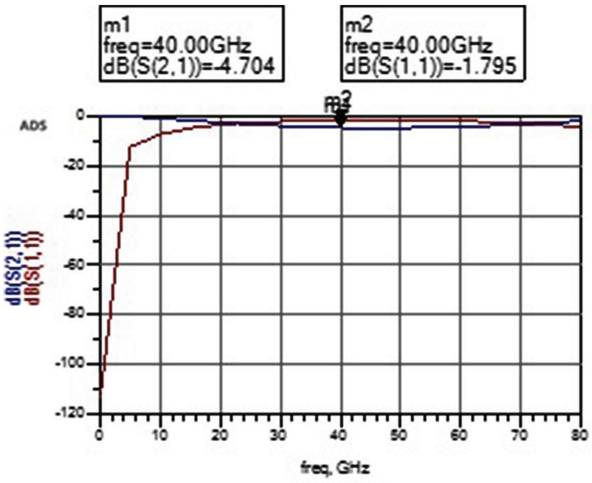

Figure 7: S-parameters of switch-up state

4.3 RF switch parameters

The electromagnetic analysis of the designed optimal switch is performed using the advance design system for wireless Communications software and equations 2 and 3. In addition, the index of dispersion (S parameter) is simulated. As illustrated in Fig.7, when the electrical voltage is not applied to the switch and the switch is off, the return loss is S_{11}=-2.54dB at the frequency of 40 GHz. Additionally, after applying the actuation voltage to the membrane surface and turning on the switch, the isolation is S_{21}=-33.18dB at the frequency of 40 GHz as shown in Fig.8.

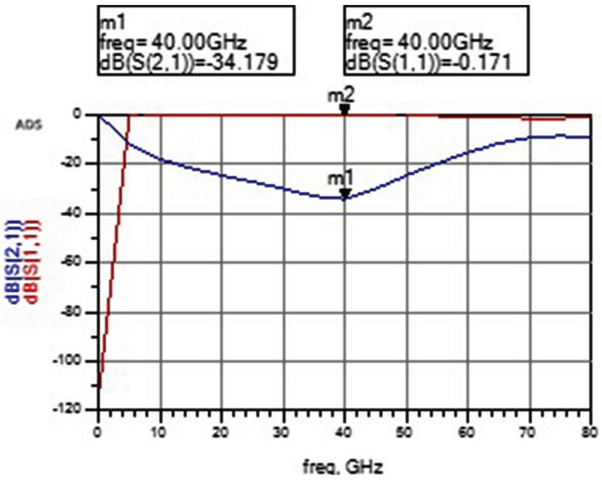

Figure 8: S-parameters of switch-down state

5 Results

The present paper developed a multi-objective model for determining the actuation voltage and insertion loss up-state and isolation down-state of an aluminium switch using a mathematical programming technique. The proposed model was solved by using the NSGA-II meta-heuristic algorithm and uti-liti algorithm. By extracting the Pareto solution set, the actuation voltage and insertion loss up-state and isolation down-state

Table 7: Comparison of developed capacitive RF-MEMS switches

	[5]	[6]	[7]	[8]	[9]	[4]	This work
V	7V	82V	23.6V	25V	3V	3.04V	2V
K	0.27N/m	-	1.43N/m	-	0.65N/m	1. 3N/m	1.213N/m
g_{gap}	1.1µm	-	3µm	3µm	2.2µm	1.397µm	1.1µm
t_d	Sio, ε_r=3.9	Sio, ε_r=3.9	AIN, ε_r=9.8	Si3N4, ε_r=6-7	Sio2, ε_r=4.99	Sio2, ε_r=4.99	Sio2, ε_r=4.99
S_{11}	3.1dB-	0.9dB-	0.68dB-	.8dB-	-	-5.6dB	-2.54dB
S_{21}	-15dB	-17dB	-35.7dB	-30dB	-	-24dB	-33.18dB
T	8.2µs	49µs	8.2µs	-	-	30µs	29.6µs

of the beam using five membranes in the form of flexure Serpentine for spring constant were reported as reported k=1.213N/M. In addition, the suitable design surfaces; including, length 45µm, width 4.5µm and thickness 1.7µm, and the number of members 4were selected to minimize the objective function of the switch. After the optimal design of the switch from the RF MEMS switch, the electrostatic pull-in voltage was calculated as 2V. The response time of the MEMS switch was about 29.6µs and the capacitance ratio was equal to 70. The return loss and isolation were S_{11}=--2.54dB and S_{21}=-33.18dB for the optimized switch at the frequency of 40 GHz.

6 Conclusion

Table 7 presents the comparison of our work with some typical developed capacitive RF-MEMS switches.

As shown in the Table 7, the designed switch has an optimal spring constant better than the previous work, and also the lower stimulation voltage and isolation and return loss due to the compromise between the parameters. As compared to the previous works, the design is remarkable and appropriate. But, generally speaking, with the presentation of the planned design and in many indicators, they exhibit their values and their superiority to other design methods that are based on trial and error.

7 References

1. Singh T (2014) Design and finite element modeling of series-shunt configuration based RF MEMS switch for high isolation operation in K???Ka band. J Comput Electron 14:167–179. https://doi.org/10.1007/s10825-014-0636-2
2. Rebeiz GM (2003) RF MEMS: Theory, Design and Technology
3. Mulloni V, Solazzi F, Resta G, et al (2014) RF-MEMS switch design optimization for long-term reliability. Analog Integr Circuits Signal Process 78:323–332. https://doi.org/10.1007/s10470-013-0220-x
4. Ma LY, Nordin AN, Soin N (2016) Design, optimization and simulation of a low-voltage shunt capacitive RF-MEMS switch. Microsyst Technol 22:537–549. https://doi.org/10.1007/s00542-015-2585-5
5. Dai CL, Chen JH (2006) Low voltage actuated RF micromechanical switches fabricated using CMOS-MEMS technique. Microsyst Technol 12:1143–1151. https://doi.org/10.1007/s00542-006-0243-7
6. Fouladi S, Mansour RR (2010) Capacitive RF MEMS Switches Fabricated in Standard 0.35- CMOS Technology. IEEE Trans Microw Theory Tech 58:478–486. https://doi.org/10.1109/TMTT.2009.2038446
7. Bartolucci G, De Angelis G, Lucibello A, et al (2012) Analytic modeling of RF MEMS shunt connected capacitive switches. J Electromagn Waves Appl 26:1168–1179. https://doi.org/10.1080/09205071.2012.710564
8. Molaei S, Ganji BA (2017) Design and simulation of a novel RF MEMS shunt capacitive switch with low actuation voltage and high isolation. Microsyst Technol 23:1907–1912. https://doi.org/10.1007/s00542-016-2923-2
9. Ya ML, Nordin AN, Soin N (2013) Design and analysis of a low-voltage electrostatic actuated RF CMOS-MEMS switch. Proc - RSM 2013 2013 IEEE Reg Symp Micro Nano Electron 41–44. https://doi.org/10.1109/RSM.2013.6706468
10. Yao JJ (2000) TOPICAL REVIEW RF MEMS from a device perspective. 10:
11. Rebeiz GM, Muldavin JB (2001) RF MEMS switches and switch circuits. IEEE Microw Mag 2:59–71. https://doi.org/10.1109/6668.969936
12. Bazaraa MS, Jarvis JJ SH (2014) Linear Programming and Network Flows
13. Pozar MD (2005) Transmission line theory. Microw Eng 49–64. https://doi.org/10.1002/0471654507.eme459
14. Ramesh S, Kannan S, Baskar S (2012) Application of modified NSGA-II algorithm to multi-objective reactive power planning. Appl Soft Comput J 12:741–753. https://doi.org/10.1016/j.asoc.2011.09.015
15. Lazic RZ (2004) Design of experiments in chemical engineering a practical guide
16. Noorollahi E, Fadai D, Ghodsipour SH, Shirazi MA (2017) Developing a new optimization framework for power generation expansion planning with the inclusion of renewable energy - A case study of Iran. J Renew Sustain Energy 9:. https://doi.org/10.1063/1.4974859
17. Jaafar H, Beh KS, Yunus NAM, et al (2014) A comprehensive study on RF MEMS switch. Microsyst Technol. https://doi.org/10.1007/s00542-014-2276-7

Arrived: 18. 01. 2019
Accepted: 17. 04. 2019